Record of Volcanism Since 7000 B.C. from the GISP2 Greenland Ice Core and Implications for the Volcano-Climate System

G. A. Zielinski,* P. A. Mayewski, L. D. Meeker, S. Whitlow, M. S. Twickler, M. Morrison, D. A. Meese, A. J. Gow, R. B. Alley

Sulfate concentrations from continuous biyearly sampling of the GISP2 Greenland ice core provide a record of potential climate-forcing volcanism since 7000 B.C. Although 85 percent of the events recorded over the last 2000 years were matched to documented volcanic eruptions, only about 30 percent of the events from 1 to 7000 B.C. were matched to such events. Several historic eruptions may have been greater sulfur producers than previously thought. There are three times as many events from 5000 to 7000 B.C. as over the last two millennia with sulfate deposition equal to or up to five times that of the largest known historical eruptions. This increased volcanism in the early Holocene may have contributed to climatic cooling.

Volcanic aerosols have an important role in the Earth's climate, beginning with their contribution to the development of the primordial atmosphere (*1*). More recently, much interest has focused on the effect of the sulfur in these aerosols on tropospheric temperature (*2*), their potential contribution to stratospheric ozone depletion (*3*), and their possible role in initiating El Niño events (*4*). Although the recent El Chichón and Mount Pinatubo eruptions illustrated that significant atmospheric effects are observable, the overall magnitude and duration of the climatic effects particularly in past times are still uncertain (*5*). One critical deficiency has been a lack of a continuous high-resolution paleovolcanic record (6) for comparison with available climatic records. In this paper we present a record of past volcanism from the present to 7000 B.C. (0 to 9000 years ago) from the ice core of the Greenland Ice Sheet Project Two (GISP2), drilled at Summit, Greenland (72.6°N, 38.5°W, and 3200 m in elevation).

The basis for our paleovolcanic record is the time series of SO_4^{2-} concentration in continuous, biyearly samples from the upper 1468 m of the core (*7*). Concentrations of SO_4^{2-} in ice cores can sharply increase independently of other ions and particularly cations that are indicators of either sea salt (Na^+) or continental dust (Ca^{2+}) (*8–10*). This excess indicates that most large spikes in SO_4^{2-} concentration reflect the deposition of volcanically derived aerosols (*9, 10*). The SO_4^{2-} time series complements and expands earlier acidity measurements (*11, 12*) that revealed the potential use of ice cores in paleovolcanic research. Concentrations of SO_4^{2-} are a direct measure of the deposition of volcanically produced H_2SO_4, which is the most important volcanic aerosol climatically, whereas the acidity record also reflects nonclimatic forcing components such as HCl and HF (*13*). Although a moderate high-latitude Northern Hemisphere eruption may deposit as much SO_4^{2-} on Greenland as a much larger equatorial or Southern Hemisphere eruption, the aerosol distribution from these large eruptions is global and therefore the continuous Greenland core provides a complete record of such events.

We determined SO_4^{2-} concentrations with an ion chromatograph (*9, 14*). The depth-age scale of the core was developed through the counting of annual signals observed in physical properties, through electrical conductivity methods (ECM), and in laser-light scattering characteristics of the ice (*15*). The ECM signal observed in the GISP2 core from several large historical volcanic eruptions (*16*), as correlated with ECM records in other ice cores from Greenland, and the identification of volcanic glass from some of these same eruptions (*17*) established distinct time lines to calibrate the annual counting. The error of the depth-age scale is 2%, or ±180 years at 7000 B.C. (9000 years ago) (*18*). The biyearly sampling of SO_4^{2-} results in an additional error of ±2 years for individual eruptions (*19*). The time lag between the eruption and deposition of aerosols in Greenland can be at least 2 years, depending on the latitude of the volcano and the season in which the eruption occurred. Longer lag times may exist for equatorial eruptions and eruptions that occur during the summer when there is less mixing between tropical and polar air masses.

We used two different approaches to identify possible volcanic events over the length of our record. The first was based on an estimation of background SO_4^{2-} concentrations by a low-tension robust spline

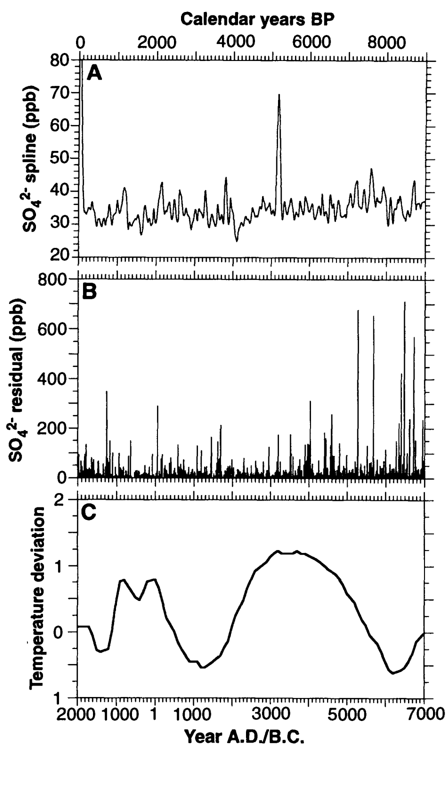

Fig. 1. (**A**) Low-tension robust spline of SO_4^{2-} concentrations from the present to 7000 B.C. (0 to 9000 years ago) in the GISP2 ice core. This curve essentially represents the trend in background SO_4^{2-} concentrations through this time period. The 150-year period of high background levels around 3100 to 3200 B.C. probably reflects a marked increase in the deposition of marine biogenic SO_4^{2-} because there is no record of such an extensive period of volcanism around that time and because individual peaks in the raw SO_4^{2-} data during this time lack the sharpness typical of volcanically derived SO_4^{2-}. Open water in the permanent sea ice (that is, a polynya) off the Greenland coast could account for this extended period of increased marine biogenic SO_4^{2-} deposition. The increase in background levels of SO_4^{2-} from anthropogenic activity over the last few centuries is also seen (*9, 10*). (**B**) Positive residuals over this same time period believed to represent the deposition of volcanically derived SO_4^{2-}. Residual values on the ordinate represent the amount of SO_4^{2-} in parts per billion above the spline value. (**C**) Composite of the postulated variation in Northern Hemisphere surface temperatures from the present to 7000 B.C. (*35*). Temperature change was determined by a deviation from the mean value at the turn of the last century.

G. A. Zielinski, P. A. Mayewski, L. D. Meeker, S. Whitlow, M. S. Twickler, M. Morrison, Glacier Research Group, Institute for the Study of Earth, Oceans and Space, University of New Hampshire, Durham, NH 03824, USA.
D. A. Meese and A. J. Gow, Cold Regions Research and Engineering Laboratory, Hanover, NH 03755, USA.
R. B. Alley, Earth Systems Science Center and Department of Geosciences, The Pennsylvania State University, University Park, PA 16802, USA.

*To whom correspondence should be addressed.

(*20*) (Fig. 1, A and B) and the selection of events with a residual value ≥25 ppb (that is, 1σ above the mean of all positive residual values) as indicative of a potential climate-forcing eruption. The second method was based on a multivariate discriminant analysis of residuals from high-tension robust splines (*21*) of all eight anion and cation series of the GISP2 record, resulting in an average discriminant function for samples containing volcanic aerosols. There is only about a 10% difference in the total number of events recorded by each method (*22*).

We compared residuals with a value of ≥25 ppb to known volcanic eruptions from A.D. 1985 to A.D. 1 (0 to 2000 years ago) (Table 1) to validate the record from the residuals. We chose this time period as a standard because volcanic events are relatively well documented (*16*) and because it contains perhaps the earliest exactly dated eruption, the A.D. 79 eruption of Mount Vesuvius that destroyed Pompeii. We primarily considered eruptions with a volcanic explosivity index (VEI) ≥4 (*23*) in our comparisons. One criterion for a VEI ≥4 rating is stratospheric injection (*23*), which, for most Northern Hemisphere eruptions and the very largest Southern Hemisphere eruptions, would favor the long-distance transport of aerosols to the Greenland ice sheet. As shown in Table 1, 57 of the 69 residual SO_4^{2-} events (85%) during the last 2000 years in the ice-core record can be matched with a known eruption. This comparison supports the inference that high SO_4^{2-} residuals have a volcanic source. However, the historical record is short in many volcanic regions, and the prehistorical record is either nonexistent or subject to the uncertainties of age-dating techniques (*16*).

Of the 69 events, 45 can be attributed to equatorial or mid-latitude Northern Hemisphere eruptions (Table 1), and 12 events are attributed to Icelandic eruptions (~20% of the identifiable eruptions). Although 12 events are undocumented, in several cases we attributed SO_4^{2-} spikes that occur in adjacent samples to a single eruption (such as Kuwae, A.D. 1459 and 1460; Ilopango, A.D. 264 and 267) (Table 1). In these particular cases, there may

Table 1. Volcanic eruptions thought to be most responsible for high SO_4^{2-} residuals (≥1σ above mean positive residual value) recorded in the GISP2 ice core over the last 2000 years. The uncertainty in the age of the eruption is also shown where applicable.

Year of Signal*	SO_4^{2-} Residual (ppb)†	Volcanic eruption with year	VEI‡
1979	25	Westdhal, Alaska, USA, 1978	3?
1971	83	Hekla, Iceland, 1970	3
1969	92	Fernandina, Galápagos, 1968	4
1965	29	Sheveluch, Kamchatka, Russia, 1964	4+
		Surtsey, Iceland, 1963	3
1956§	18	Bezymianny, Kamchatka, Russia, 1956	5
1924	32	Raikoke, Ryukyu Islands, Japan, 1924	4
		Iriomote-Jima, Japan, 1924	4?
1917	32	Katla, Iceland, 1918	4
1912	67	Katmai, Alaska, USA, 1912	6
1902	41	Santa Maria, Guatemala, 1902	6
		Soufriere, St. Vincent, 1902; Pelee, Martinique, 1902	4
1883	46	Krakatau, Indonesia, 1883	6
1854‖	27	Sheveluch, Kamchatka, Russia, 1854	5
		Chikurachki-Tatarinov, Kurile Islands, 1853	5?
1831	68	Babuyan, Philippines, 1831	4
1830	52	Kliuchevskoi, Kamchatka, Russia, 1829	4?
1815	94	Tambora, Indonesia, 1815	7
1809	67	Unknown	?
1781	134	Laki, Iceland, 1783; Asama, Japan, 1783	4
1765	35	Hekla, Iceland, 1766	4
1737	32	Tarumai, Japan, 1739	5
1727	25	Oræfajokull, Iceland, 1727	4
1695	39	Komaga-Take, Japan, 1694	4
1693	29	Hekla, Iceland, 1693	4
1667	32	Tarumai, Japan, 1667	5
1645§	20	Long Island, New Guinea, 1660 ± 20	6
1641	81	Awu, Indonesia, 1641; Komaga-Take, Japan, 1640	5?
1604	61	Momotombo, Nicaragua, 1605	4
		Huaynaputina, Peru, 1600	5?
1588	34	Kelut, Java, 1586	5?
1587	72	Colima, Mexico, 1585	4
1570	28	Billy Mitchell, Solomon Islands, 1580 ± 30	6
1483	34	Mount St. Helens, Washington, USA, 1482	4?
		Kelut, Java, 1481	4
1478	63	Mount St. Helens, Washington, USA, 1479	5
1460	66	Kuwae, Vanuatu, 1450 ± ?	?
1459	56	Kuwae, Vanuatu, 1450 ± ?	?
1344	54	Hekla, Iceland, 1341	3
1328	33	Cerro Bravo, Columbia, 1325 ± 75	4
1285	44	Unknown; Asama, Japan, 1281	4
1259	349	Unknown (possibly El Chichón, Mexico)	?
1229	78	Unknown	?
1227	34	Unknown	?
1205	32	Oshima, Japan, 1200 ± 50	4
1194	61	Oshima, Japan, 1200 ± 50	4
1175	148	Krafla, Iceland, 1179 ± 2	4?
1103	100	Hekla, Iceland, 1104	4
1026	43	Baitoushan, China, 1010 ± 50	7
		Billy Mitchell, Solomon Islands, 1030 ± 25	5+
939	33	Eldgjá, Iceland, 934 ± 2	4
938	98	Eldgjá, Iceland, 934 ± 2	4
936	65	Eldgjá, Iceland, 934 ± 2	4
915‖	26	Towoda, Japan, 915	5
902	40	Bardarbunga, Iceland, 900?; Tolbachik, Kamchatka, Russia, 900?	4
		Ksudach, Kamchatka, Russia, 900 ± 50	5
900	39	Same as in 902	
875	33	Kaimon, Japan, 874	4?
853‖	29	Furnas, Azores, 840 ± 100	4
823	42	Unknown	?
822	41	Unknown	?
767	28	Cerro Bravo, Columbia, 750 ± 150; Oshima, Japan, 750 ± 50	4
757‖	27	Oshima, Japan, 750 ± 50	4
702‖	26	Bezymianny, Kamchatka, Russia, 700 ± 50	4?
		Bona-Churchill, Alaska, USA, 700 ± 200	6
696‖	31	Same as in 702; unknown	?
695	34	Same as in 702; unknown	?
691	87	Unknown	?
639	149	Unknown	?
508‖	27	Oshima, Japan, 500 ± 200	4
		Sheveluch, Kamchatka, Russia, 500 ± 50	5
472	29	Vesuvius-Pollena, Italy, 472	4
436‖	27	Opala, Kamchatka, Russia, 430?	5+
267	49	Unknown; Ilopango, El Salvador, 260 ± 100	6
264	48	Ilopango, El Salvador, 260 ± 100	6
181§	20	Taupo, New Zealand, 177 ± 10	6
161‖	32	Ksudach, Kamchatka, Russia, 155 ± 100	6
152	45	Ibusuki, Japan, 150?	4
77	95	Vesuvius, Italy, 79	5

*Year of signal in ice core based on interpolated age of each sample from spline. The year of signal is ±2, on the basis of a biyearly sampling scheme. †Residual values are not directly related to the amount of atmospheric loading of the particular eruption or eruptions due to the effects of latitude of eruption on the amount of SO_4^{2-} deposition in Greenland. ‡VEI from (*16*). VEI is queried when not given in (*16*) or when magnitude is uncertain. §Events that did not meet the residual criteria but were identified by discriminant analysis. ‖Events that met the criteria for residuals but were not identified with the discriminant analysis.

have been an unknown eruption that occurred within 1 or 2 years of the documented eruption. Many of the major events that we identified in Table 1 (such as Tambora, A.D. 1815) have been identified in other ice cores from Greenland (*8, 11, 12*). We also identified other large mid-latitude (such as Mount St. Helens, A.D. 1479 and 1482) and equatorial (such as Kuwae, A.D. 1459) eruptions that either were not observed or not named in these other cores (*24*). In some cases, these identifications must be regarded as tentative, but in others the presence of a single large SO_4^{2-} residual in the time range of a major explosive eruption allows confident correlation.

We estimated the stratospheric loading of several large equatorial eruptions over the past 2000 years in the GISP2 core (*25*). The results of this comparison suggest that H_2SO_4 loading values for the combined

Table 2. Dates of events with residuals ≥25 ppb (1σ above mean positive residual value) for each century between 1 B.C. and 7000 B.C. The SO_4^{2-} residual values (given in parentheses, in parts per billion) are not directly related to the amount of atmospheric loading of the particular eruption because of the effects of latitude of eruption on the amount of SO_4^{2-} deposition in Greenland. Possible eruptions with VEI ≥5 (*16*) responsible for specific events are also given, although eruptions dated by ^{14}C have not been corrected to calendar years. Legend of events: a, Sheveluch, Kamchatka, Russia (50 ± ? B.C.); b, Vulcano, Italy (183 B.C.); c, Okmok, Alaska, USA (450 ± 200 B.C.); d, Krafla, Iceland (550 ± ? B.C.); e, Yantarni, Alaska, USA (800 ± 500 B.C.); f, Bardarbunga (Veidivotn), Iceland (1150 ± 100 B.C.); g, Aniakchak, Alaska, USA (1480 ± 10 B.C.); h, Santorini (Minoan eruption), Greece (1623–1627 B.C.); i, Long Island, New Guinea (2040 ± 100 B.C.); j, Hekla (H-4), Iceland (2310 ± 20 B.C.); k, Black Peak, Alaska, USA (2485 ± 300 B.C.); l, Akutan, Alaska, USA (3250 ± 200 B.C.); m, Towada, Japan (3450 ± 150 B.C.); n, Kikai, Ryuku, Japan (4350 ± ? B.C.); o, Avachinsky, Kamchatka, Russia (4400 ± ? B.C.); p, Masaya, Nicaragua (4550 ± ? B.C.); q, Mazama, Oregon, USA (4895 ± 50 B.C.); r, Hekla (H-5), Iceland (5050 ± ? B.C.), and Hangar, Kamchatka, Russia (5040 ± 75 B.C.); s, Kizimin, Kamchatka, Russia (5300 ± 300 B.C.); t, Tao-Rusyr, Kurile Islands (5550 ± ? B.C.); u, Karymsky, Kamchatka, Russia (5700 ± 50 B.C.); v, Vesuvius, Italy (5960 ± 100 B.C.); w, Pauzhetka, Kamchatka, Russia (6220 ± 150 B.C.); x, Bardarbunga (Veidivotn), Iceland (6650 ± 50 B.C.), and Towada, Japan (6650 ± 300 B.C.).

Period (years B.C.)	Year B.C.	Period (years B.C.)	Year B.C.
1–100	44 (30), 54 (291)[a], 99 (26)	3501–3600	3518 (174)[m], 3529 (35), 3541 (97), 3588 (86)
101–200	102 (27), 149 (30), 151 (76), 156 (44), 170 (28), 174 (29), 178 (42), 180 (93)[b]	3601–3700	3649 (30), 3651 (30)
201–300	229 (38), 253 (50), 256 (34), 265 (26), 292 (30)	3701–3800	3720 (38), 3734 (49), 3763 (30), 3775 (76), 3793 (30)
301–400	365 (58)	3801–3900	3815 (32), 3880 (54)
401–500	406 (81)[c], 413 (64)[c], 476 (28), 490 (26)	3901–4000	3905 (134), 3906 (69), 3925 (67), 3927 (45), 3957 (72), 3977 (137)
501–600	502 (39), 585 (132)[d]	4001–4100	4008 (27), 4010 (133), 4035 (313), 4039 (148), 4063 (38), 4078 (31), 4098 (36), 4099 (57)
601–700	611 (41), 618 (32), 621 (44), 663 (55), 674 (35), 690 (35)	4101–4200	None
701–800	727 (31), 737 (74)[e], 740 (30), 776 (29)	4201–4300	4267 (71)[n]
801–900	864 (43)	4301–4400	4395 (38)
901–1000	962 (35)	4401–4500	4411 (183)[o], 4436 (67)[o], 4447 (159)[o], 449 (42)
1001–1100	1015 (25), 1084 (129)[f]	4501–4600	4558 (26), 4564 (132)[p], 4596 (257)
1101–1200	1128 (28), 1157 (26), 1190 (30), 1192 (110)[f]	4601–4700	4616 (69), 4626 (28), 4627 (89), 4641 (50), 4667 (89), 4689 (310)
1201–1300	1284 (44)	4701–4800	4731 (33), 4753 (30), 4764 (30), 4774 (49)
1301–1400	1327 (46), 1337 (27)	4801–4900	4803 (141)[q], 4893 (31)
1401–1500	1442 (57), 1454 (164)[g], 1457 (67)[g], 1459 (104)[g]	4901–5000	4911 (49), 4941 (40), 4988 (93)[r], 4997 (27)
1501–1600	1577 (29), 1594 (30), 1600 (40)	5001–5100	5060 (33)
1601–1700	1602 (58), 1623 (145)[h], 1669 (78)[h], 1695 (213)	5101–5200	5127 (34), 5150 (29), 5152 (37)
1701–1800	1715 (26)	5201–5300	5209 (67), 5237 (44), 5240 (34), 5245 (38), 5277 (677)[s], 5279 (404)[s]
1801–1900	1811 (28), 1818 (30), 1850 (26), 1864 (39), 1891 (46)	5301–5400	5348 (45), 5361 (59), 5391 (32)
1901–2000	1919 (35), 1936 (49), 1948 (38), 1991 (74)[i], 1994 (31)	5401–5500	5456 (49)
2001–2100	2034 (42)	5501–5600	5519 (36), 5521 (129)[t], 5561 (27), 5588 (60)
2101–2200	2143 (34), 2167 (31)	5601–5700	5629 (65), 5638 (45), 5640 (44), 5675 (168), 5676 (654), 5688 (81)[u]
2201–2300	2207 (26), 2294 (63)	5701–5800	5751 (28), 5776 (33), 5781 (76)
2301–2400	2304 (47), 2310 (80)[j], 2398 (41)	5801–5900	5860 (50), 5870 (42)
2401–2500	2500 (49)	5901–6000	5918 (33), 5921 (42), 5954 (69)[v], 5995 (115)[v]
2501–2600	None	6001–6100	6007 (44), 6100 (28)
2601–2700	2617 (68)[k], 2619 (41), 2656 (40), 2660 (35)	6101–6200	6102 (37), 6112 (44), 6115 (56), 6160 (38), 6182 (39), 6194 (31)
2701–2800	None	6201–6300	6218 (40), 6258 (35), 6264 (48), 6271 (79)[w], 6273 (150)[w], 6296 (29)
2801–2900	2815 (66)	6301–6400	6338 (222), 6341 (36), 6354 (32), 6360 (92), 6396 (130), 6398 (424)
2901–3000	2906 (31), 2920 (30), 2955 (72), 2958 (124)	6401–6500	6440 (57), 6470 (154), 6476 (710)
3001–3100	None	6501–6600	6522 (37), 6539 (40), 6555 (101), 6560 (64)
3101–3200*	3154 (29), 3173 (65), 3177 (46), 3179 (62), 3181 (48), 3184 (42), 3188 (42), 3190 (41), 3192 (27)	6601–6700	6604 (33), 6614 (240)[x]
3201–3300	3201 (175)[l], 3258 (66)[l]	6701–6800	6714 (29), 6718 (27), 6720 (396)[x], 6722 (572)[x], 6766 (153), 6774 (33), 6785 (47), 6797 (29)
3301–3400	3340 (31), 3350 (27)	6801–6900	6814 (33), 6821 (31), 6828 (34), 6845 (38)
3401–3500	3402 (32), 3489 (26)	6901–7000	6911 (37), 6931 (42), 6946 (27), 6951 (55), 6955 (236), 6973 (71)

*High residuals during the latter part of this century are probably due to an increase in the amount of biogenic SO_4^{2-} deposited at the GISP2 site and not to a volcanic source. See explanation in the legend to Fig. 1.

early 1640 and early 1600 eruptions, and possibly the Babuyan eruption [A.D. 1831 (*26*)], are only exceeded by the Tambora (1815) and 1259 events. High sulfur loading from multiple eruptions such as in the 17th century may have cooled the climate during those particular time periods (*12, 27*), but more work is needed to evaluate the size and characteristics of these less well known eruptions. A signal at A.D. 181 in the discriminant analysis (Table 1) may be related to the deposition of aerosols from the ~A.D. 177 ultraplinian eruption of Taupo, New Zealand (*28, 29*). The estimated column height of 55 km for the Taupo eruption (*28*) may have enabled aerosols to be distributed globally despite its Southern Hemisphere location [39°S (*30*)].

In contrast to the record over the last 2000 years, many of the 232 events recorded from 1 B.C. to 7000 B.C. (2000 to 9000 years ago) cannot easily be matched to a known volcanic eruption. For instance, we have listed 26 large eruptions [VEI ≥5 (*16*)] that may be associated with SO_4^{2-} residuals older than 1 B.C. (2000 years ago) (Table 2). An additional 40 known eruptions with a VEI of 4 (*16*) could also be attributed to SO_4^{2-} residuals over that time period, resulting in the possible identification of only 25 to 30% of the large sulfur-producing eruptions that occurred from the early to middle Holocene (*31*).

Several well-known eruptions may be tentatively matched to an SO_4^{2-} signal between 1 B.C. and 7000 B.C. (2000 to 9000 years ago). For example, the high SO_4^{2-} residual at 1623 B.C. (Table 2) may be from the Santorini (Minoan) eruption thought to have occurred around 1626 to 1628 B.C. (*32*). Similarly, the high SO_4^{2-} residual at 4803 B.C. (Table 2) may be related to the cataclysmic eruption of Mount Mazama (Crater Lake). The potential amount of atmospheric loading of the Mazama eruption, based on the SO_4^{2-} residual of 148 ppb, is probably comparable to that of the Tambora eruption (94 ppb), in consideration of the difference in latitude of the two volcanoes.

From 5000 to 7000 B.C. (7000 to 9000 years ago), 18 events with residuals greater than 100 ppb (*33*) are evidenced (Fig. 1B), compared to only five events of similar magnitude over the last 2000 years. The early Holocene is thought to be characterized by a high input of solar radiation to the Northern Hemisphere (*34*), but increased volcanic activity could have contributed to a brief period of cooling suggested by the composite record of Northern Hemisphere temperature fluctuations (*35*) (compare Figs. 1B and 1C). Comparisons with other GISP2 records, such as for annual accumulation, do indicate cooler conditions over Greenland around 6000 to 7000 B.C. (8000 to 9000 years ago).

This apparent increase in the atmospheric loading of SO_4^{2-} during the early Holocene may be the result of increased volcanic activity in either Iceland, Kamchatka, or Alaska, or quite possibly in all three regions. Certainly the high amount of SO_4^{2-} deposition for individual events recorded at the GISP2 site would favor a more proximal source like Iceland. However, Kamchatkan and Alaskan volcanism would load the atmosphere directly upwind from the Greenland ice sheet. The early Holocene volcanic history of these regions has only recently been studied (*36*), and much more work is needed. Increased volcanic activity originating in these high-latitude sites during the millennia following deglaciation could support the idea that isostatic adjustment following deglaciation and the subsequent response of magma chambers to these changes in crustal stresses may lead to a period of more explosive volcanism (*37*).

REFERENCES AND NOTES

1. P. Warneck, *Chemistry of the Natural Atmosphere* (Academic Press, San Diego, 1988).
2. See M. R. Rampino, R. B. Stothers, S. Self, *Nature* **313**, 272 (1985); M. R. Rampino, S. Self, R. B. Stothers, *Annu. Rev. Earth Planet. Lett.* **16**, 73 (1988), and references therein. Also see D. Rind, N. K. Balachandran, R. Suozzo, *J. Clim.* **5**, 189 (1992).
3. D. J. Hofmann and S. Solomon, *J. Geophys. Res.* **94**, 5029 (1989).
4. P. Handler, *J. Volcanol. Geotherm. Process.* **37**, 233 (1989).
5. S. Self and M. R. Rampino, *Eos* **69**, 74 (1988).
6. R. S. Bradley and P. D. Jones, in *Climate Since A.D. 1500*, R. S. Bradley and P. D. Jones, Eds. (Routledge, New York, 1992), pp. 606–622.
7. Higher base-line concentrations of SO_4^{2-} below this depth (that is, before 7000 B.C.) may be a result of the deposition of continental salts; thus, the volcanic signal is complicated.
8. M. Legrand and R. J. Delmas, *Nature* **327**, 671 (1987); W. B. Lyons *et al.*, *Ann. Glaciol.* **14**, 176 (1990).
9. P. A. Mayewski *et al.*, *Science* **261**, 195 (1993).
10. P. A. Mayewski *et al.*, *J. Geophys. Res.* **98**, 12839 (1993).
11. C. U. Hammer, H. B. Clausen, W. Dansgaard, *Nature* **288**, 230 (1980).
12. T. J. Crowley, T. A. Criste, N. R. Smith, *Geophys. Res. Lett.* **20**, 209 (1993).
13. K. Taylor *et al.*, *J. Glaciol.* **38**, 325 (1992).
14. P. A. Mayewski *et al.*, *Atmos. Environ.* **21**, 863 (1987); P. A. Mayewski *et al.*, *Nature* **346**, 554 (1990); F. Buck, *J. Chromatogr.* **594**, 225 (1992).
15. D. Meese *et al.*, *U.S. Army Cold Reg. Res. Eng. Lab. Rep.*, in press.
16. The age of documented volcanic eruptions primarily comes from T. Simkin and L. Siebert, *Volcanoes of the World* (Hutchinson Ross, Stroudsburg, PA, 1981), a 1984 supplement to that original work, and revised listings for the forthcoming second edition.
17. R. J. Fiacco *et al.*, *Quat. Res.* **39**, 267 (1993); J. M. Palais, M. S. Germani, G. A. Zielinski, *Geophys. Res. Lett.* **19**, 801 (1992).
18. R. B. Alley *et al.*, *Nature* **362**, 527 (1993).
19. Major ion chemistry was measured for approximately biyearly samples over the entire length of the GISP2 core (*9, 10*). We evaluated several volcanic sections at a subannual resolution to confirm the age of the volcanic SO_4^{2-} signal and to locate and identify volcanic glass (*17*).
20. P. Bloomfield and W. L. Steiger, *Least Absolute Deviation* (Birkhäuser, Boston, 1983).
21. W. J. Krzanowki, *Principles of Multivariate Analysis* (Oxford Univ. Press, London, 1988).
22. The discriminant function picked all the events meeting our residual criteria of 25 ppb except, on average, less than one event per 100 years. About one event per 1000 years was picked by the discriminant function despite a residual ≤25 ppb. Residuals were ≥15 ppb in all of these cases.
23. C. G. Newhall and S. Self, *J. Geophys. Res.* **87**, 1231 (1982).
24. Evidence of a large volcanic eruption in the A.D. 1450s has been seen in many ice cores, but recently presented radiocarbon ages (J. P. Eissen, M. Monzier, C. Robin, paper presented at the International Association of Volcanology and Chemistry of The Earth's Interior (IAVCEI) General Assembly, Canberra, Australia, 25 September to 1 October, 1993) enabled us to match our SO_4^{2-} signal with the Kuwae eruption.
25. G. A. Zielinski *et al.*, paper presented at the IAVCEI General Assembly, Canberra, Australia, 25 September to 1 October, 1993. We used the technique developed by H. B. Clausen and C. U. Hammer [*Ann. Glaciol.* **10**, 16 (1988)] to estimate the amount of stratospheric H_2SO_4 produced by a particular eruption. This procedure assumes that the amount of H_2SO_4 produced from the eruption and eventually deposited on the Greenland ice sheet is similar to that of material injected into the stratosphere by nuclear bomb testing of a known location and magnitude.
26. Brightly colored sunsets and the appearance of a dry fog in the Northern Hemisphere during the early 1830s, as compiled by H. H. Lamb [*Philos. Trans. R. Soc. London Ser. A.* **266**, 52 (1970)] were similar to those following the A.D. 1783 eruption of Laki. This similarity suggests that there was a large sulfur-producing eruption in the Northern Hemisphere, quite possibly Babuyan. J. K. Angell and J. Korshover [*J. Clim. Appl. Meteorol.* **24**, 937 (1985)] and S. Self, M. R. Rampino, and M. J. Carr [*Bull. Volcanol.* **52**, 57 (1989)] emphasized that temperatures in some places in the Northern Hemisphere were declining for several years before the explosive eruption of Cosiguina in 1835, further suggesting the possibility of a very large eruption in the early 1830s.
27. K. R. Briffa *et al.*, *Clim. Dyn.* **7**, 111 (1992); K. R. Briffa *et al.*, *J. Climatol.* **5**, 735 (1992).
28. G. P. L. Walker, *J. Volcanol. Geotherm. Res.* **8**, 59 (1980).
29. P. C. Froggatt and D. J. Lowe, *N. Z. J. Geol. Geophys.* **33**, 89 (1990).
30. C. U. Hammer [*Jökull* **34**, 51 (1984)] indicated that one possible source for a visible dust layer around A.D. 186 in the Dye 3 core may be tephra from the Taupo eruption because of the extreme height of the eruption cloud. However, it is more likely that H_2SO_4 aerosols, rather than the coarser-sized tephra component, would be carried to high latitudes of the Northern Hemisphere.
31. A list of the events with a VEI of 4 that may be matched to SO_4^{2-} residuals from 1 B.C. to 7000 B.C. may be obtained from the authors.
32. Although tree-ring studies by V. C. LaMarche Jr. and K. K. Hirschboeck [*Nature* **307**, 121 (1984)] and by M. G. L. Baillie and M. A. R. Munro [*ibid.* **332**, 344 (1988)] suggested that Santorini erupted during the 1620s B.C., D. M. Pyle [in *Chronology*, vol. 3 of *Thera and the Aegean World III*, D. A. Hardy and A. C. Rewfrew, Eds. (The Thera Foundation, London, 1990), pp. 167–173] pointed out that there is still no direct evidence to place definitively the date of the eruption as during that decade. Pyle also suggested that the amount of sulfur produced by the Santorini eruption may have been similar to that produced by Krakatau (A.D. 1883); thus, there was a low sulfur/total volume erupted ratio. If that suggestion is true, one of the smaller SO_4^{2-} residuals in the 1600s B.C. may be from the Santorini eruption.
33. A residual of 100 ppb is almost 5σ above the mean positive residual value. For comparison,

residuals for high sulfur-producing events like the equatorial Tambora eruption (A.D. 1815) and the Icelandic Laki eruption (A.D. 1783) are 94 ppb and 134 ppb, respectively. Note that SO_4^{2-} residuals for three events between 5000 and 7000 B.C. exceed 650 ppb.
34. L. Starkel, *Holocene* **1**, 234 (1991).
35. Taken from J. A. Eddy and R. S. Bradley, *Earthquest* **5** (insert) (1991), as modified from J. T. Houghton, G. J. Jenkins, J. J. Ephraums, *Climate Change, The IPCC Scientific Assessment* (Cambridge Univ. Press, Cambridge, 1990).
36. G. E. Sigvaldason, K. Annertz, M. Nilsson, *Bull. Volcanol.* **54**, 385 (1992); O. A. Braitseva *et al.*, *Quat. Int.* **13/14**, 177 (1992).
37. E. W. Grove, *Int. Assoc. Volcanol. Symp.* **1976**, 88 (1976); M. R. Rampino, S. Self, R. W. Fairbridge, *Science* **206**, 826 (1979).
38. We thank the Polar Ice Coring Office (University of Alaska), GISP2 Science Management Office (University of New Hampshire), and the 109th Air National Guard. Supported by the U.S. National Science Foundation Office of Polar Programs.

20 December 1993; accepted 15 March 1994

Seven Million Years of Glaciation in Greenland

H. C. Larsen, A. D. Saunders, P. D. Clift,* J. Beget, W. Wei, S. Spezzaferri, ODP Leg 152 Scientific Party†

Glacial till, glaciomarine diamictites, and ice-rafted detritus found in marine cores collected off the shore of southeast Greenland record multiple Late Cenozoic glaciations beginning in the Late Miocene. Distinct rock assemblages and seismic stratigraphic control correlate the diamictites with glaciation of the southeast Greenland margin. Glaciers advanced to the sea during several intervals in the Pliocene and Pleistocene. North Atlantic glaciation may have nucleated in southern Greenland rather than further north because of the high mountains and the high levels of precipitation in this region.

The Greenland Ice Sheet (GIS) is the only continental ice sheet in the Northern Hemisphere in the present interglacial period, but little is known about when it formed or its long-term history. Ice cores from the GIS show that an ice sheet was present during the last 200,000 years (*1*). Glacial sediments at two localities on Greenland are thought to have been deposited during latest Pliocene time, 1.8 to 2.0 million years ago (Ma) (*2, 3*). The earliest firm evidence of glaciation in the North Atlantic area has been from Iceland. There, glacial sediments date from 3.1 Ma (*4*), but glaciers there may not have grown large enough to reach the sea until 2.0 Ma (*5*). The earliest occurrence of abundant ice-rafted detritus (IRD) found widely in North Atlantic marine cores dates to about 2.4 Ma (*6–8*), but it is not known if ice sheets on Greenland were a source for this debris or if glaciers existed on Greenland at even earlier times. Low concentrations of fine-grain IRD have been reported from marine cores off mid-Norway and suggest that some North Atlantic glaciation could date back as early as 5.45 Ma (*8*). However, it has also been suggested that before 2.4 Ma, any glaciers in the North Atlantic area were too small to reach the sea (*5*). Hence, there is considerable uncertainty with regard to the location and timing of early glaciation within the North Atlantic.

Ocean Drilling Program, Science Operations, Texas A&M University Research Park, 1000 Discovery Drive, College Station, TX 77845–9547, USA.

*To whom correspondence should be addressed.
†The names of the members of the ODP Leg 152 Scientific Party are given in (*37*).

During Ocean Drilling Program (ODP) Leg 152, a transect of six sites (ODP sites 914 to 919) was drilled, extending from 40 to 185 km east of the southeast coast of Greenland (Fig. 1). Four sites (sites 914 to 917) were located on the continental shelf in a 500-m-deep trough, and two deep-water sites (sites 918 and 919) were located below the shelf break, 40 and 115 km seaward of the mouth of the trough, respectively. All sites are within the present-day limit of icebergs from the highly productive southeast Greenland coast (9). These marine cores contain an unusually complete record of glaciations of southeast Greenland (Fig. 2). The data show that substantial glaciation in Greenland began as early as 7 Ma in the Late Miocene following a relatively mild climate during the Middle Miocene.

The most complete record of Miocene and Pliocene glaciations was obtained at ODP site 918, drilled in 1800 m of water 110 km from the coast of Greenland (Figs. 1 and 2). The upper 550 m of sediment at the 1310-m-deep site 918 contains abundant silts and muds, within which numerous, typically granule- to pebble-size gravel clasts, but also occasionally cobble- to even boulder-size clasts, are suspended. In addition, a number of more massive, 0.3- to 10.0-m-thick beds of poorly sorted, ungraded silt, sand, and angular gravel are present (Fig. 2). The two types of sediments are interpreted as follows: (i) hemipelagic sediment and turbidites with discrete occurrences both of more fine grain IRD and larger dropstones and (ii) more massive glaciomarine diamictons. Both sediment types, therefore, reflect glacial, although variable, conditions within the source area. Indeed, intervals up to 40 m thick without macroscopic IRD exist in cores from site 918. The diamictons show relatively high magnetic susceptibility and high bulk density relative to the intercalated marine sediments. Some of these layers may be correlative with the extensive Heinrich layers of glaciomarine sediment described elsewhere in the North Atlantic, but most of the diamictite horizons are older than any previously recognized Heinrich layers (*10*).

The IRD and dropstones were present in situ, in places actually cored through, in undisturbed sediment cores for which the possibility of down-hole contamination with clasts can be excluded. However, the possibility exists that dropstones were transported within mass flows from unstable accumulations of glacial sediments of the

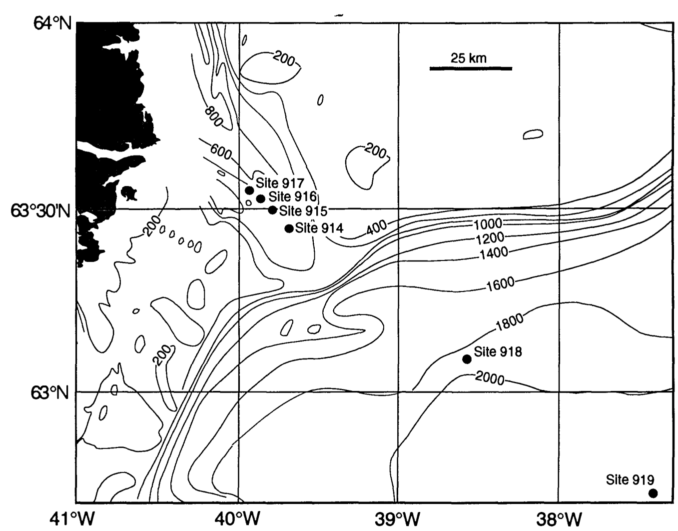

Fig. 1. Location of ODP sites 914, 915, 916, and 917 on the east Greenland shelf, and sites 918 and 919 within the deep Irminger basin. ODP site 919 lies about 75 km east of site 918. Depth values are given in meters.